A New Wavelet-Based Mode Decomposition for Oscillating Signals and Comparison with the Empirical Mode Decomposition

Adrien Deliège and Samuel Nicolay

Abstract We introduce a new method based on wavelets (EWMD) for decomposing a signal into quasi-periodic oscillating components with smooth time-varying amplitudes. This method is inspired by both the "classic" wavelet-based decomposition and the empirical mode decomposition (EMD). We compare the reconstruction skills and the period detection ability of the method with the well-established EMD on toys examples and the ENSO climate index. It appears that the EWMD accurately decomposes and reconstructs a given signal (with the same efficiency as the EMD), it is better at detecting prescribed periods and is less sensitive to noise. This work provides the first version of the EWMD. Even though there is still room for improvement, it turns out that preliminary results are highly promising.

Keywords Wavelets · Wavelet mode decomposition · Empirical mode decomposition · Continuous wavelet transform · ENSO index

1 Introduction

The aim of this paper is to provide and apply a new mode decomposition method using a wavelet-based approach. This decomposition has been introduced in [1]; we now improve it to develop a simple yet powerful mode decomposition method that we call empirical wavelet mode decomposition (EWMD). The basic idea is to extract successively "quasi-periodic" oscillating components from the continuous wavelet transform of the original signal. Each component is associated to a mean frequency but, unlike the Fourier transform, this decomposition does not lead to pure cosines: the amplitudes and frequencies slowly evolve through time. This allows to

A. Deliège(✉) · S. Nicolay
Department of Mathematics (B37), University of Liège,
Allée de la découverte 12, 4000 Liège, Belgium
e-mail: {adrien.deliege,s.nicolay}@ulg.ac.be

S. Latifi (ed.), *Information Technology New Generations*,
Advances in Intelligent Systems and Computing 448,
DOI: 10.1007/978-3-319-32467-8_83

drastically decrease the number of terms needed to accurately rebuild the signal by taking into account only the terms carrying most of the information. By doing so, the reconstructed signal resolves the main variations of the original one without taking the noise into account. For a detailed description of the theory of continuous wavelet transforms and analogies with the Fourier transform, the reader is referred to e.g. [2, 3, 4]. Let us add that several wavelet-based mode decomposition methods have been developed in recent years (see e.g. [5] and references therein). We do not intend to write a review of these techniques nor to compare our results with these studies in the present paper.

In this work, we compare the skills of the EWMD with those of the famous empirical mode decomposition (EMD) (see e.g. [6, 7, 8]). This method has proven to be well-suited for the analysis of nonlinear and nonstationary signals, despite its lack of mathematical background. It allows to decompose accurately a signal into a finite (often small) number of modes, called intrinsic mode functions (IMFs) without leaving the time domain. The basic idea of the EMD is simple and consists in the following steps. First, compute $h = f - m$ where f is the signal and m is the mean of the upper and lower envelopes of f, then repeat the process with h instead of f until h is considered to be an IMF i_1. Compute $f_1 = f - i_1$ and repeat the whole process with f_1 instead of f to obtain the next IMF i_2, then compute $f_2 = f_1 - i_2$, etc. More details can be found in e.g. [6, 7, 8]. We found that the idea of extracting one component at a time, then subtracting it from the remaining data was appealing because it could reveal components that are overshadowed by the dominant modes of the signal. As explained in the next section, this idea combined with the wavelet decomposition provided in [1] led us to this first version of the EWMD. Usual criticism made about the EMD is its lack of solid theoretical background, the high sensitivity to noise, and the inability of separating modes with frequencies close to each other but with a large difference in amplitudes. Even though this mode-mixing problems and the robustness to noise have been improved (to the detriment of computational resources) in several revisions of the EMD, such as the Ensemble EMD (EEMD [9]) and Complete Ensemble Empirical Mode Decomposition with Adaptive Noise (CEEMDAN [10]), the original EMD is not outdated and is still a good starting point for assessing the quality of a new mode decomposition method.

2 Method

In this section we describe step-by-step our empirical wavelet mode decomposition. The wavelet ψ used in this study is a Morlet-like wavelet with exactly one vanishing moment ([1]):

$$\psi(t) = \frac{e^{i\Omega t}}{2\sqrt{2\pi}} e^{-\frac{(2\Omega t+\pi)^2}{8\Omega^2}} \left(e^{\frac{\pi t}{\Omega}} + 1 \right) \tag{1}$$

with $\Omega = \pi\sqrt{2/\ln 2}$. The Fourier transform of ψ is given by

$$\hat{\psi}(\omega) = \sin\left(\frac{\pi\omega}{2\Omega}\right) e^{\frac{-(\omega-\Omega)^2}{2}} . \tag{2}$$

The decomposition procedure explained below is largely inspired by the wavelet mode decomposition in [1] but has an added feature of the empirical mode decomposition: extracting only one component then subtracting it from the signal and iterating the process. The successive steps of the EWMD are the following.

a) Perform the continuous wavelet transform of the signal f:

$$Wf(a,t) = \int f(x)\bar{\psi}\left(\frac{x-t}{a}\right)\frac{dx}{a} \tag{3}$$

where ψ is the chosen wavelet, $\bar{\psi}$ is the complex conjugate of ψ, t stands for the time (position) parameter, and $a > 0$ is the scale parameter.

b) Compute the wavelet spectrum Λ associated to f:

$$\Lambda(a) = E\,|Wf(a,.)| \tag{4}$$

where E denotes the mean over time. Then look for the scale a^* at which Λ reaches its global maximum.

c) Extract the component related to a^*:

$$|Wf(a^*,t)| \cos(\arg Wf(a^*,t)) . \tag{5}$$

d) Subtract this component from f to get, say, f', and repeat steps (a) to (d) with f' instead of f.

e) For now, we stop the process when the extracted components are not relevant anymore. More precisely, in this paper, we decided to stop the process when $\Lambda(a^*) < 0.15$. A more adequate data-driven stopping criterion should still be found. The sum of the components successively extracted is an accurate reconstruction of f, though a slight vertical rescaling can be performed to minimize the root mean square error (RMSE) with f (this will also be done with the EMD).

If we denote by $c_1, c_2, ..., c_K$ the components successively extracted with the EWMD (i.e. these components are the counterparts of the IMFs of the EMD), then the signal $c_0 = f - \sum_{k=1}^{K} c_k$ is considered as the remaining noise and therefore the decomposition of f can be completed with this noisy component:

$$f = \sum_{k=0}^{K} c_k . \tag{6}$$

Similarly to the EMD, and contrary to the method presented in [1], where there is no iterative process, i.e the components are extracted from the local maxima of the spectrum, the procedure described above extracts one component at a time. This has the advantage of unveiling components that are easily hidden by dominant modes. Also, the components successively extracted here are ordered following their energy level, while they are sorted according to their frequency with the EMD (which always gives a few noisy IMFs to start with). Consequently, more adequate data-driven stopping criteria could be based on the energy level of the component to extract.

Let us note that, in the following, the comparison between a reconstructed signal and the original one is made via two indicators: the RMSE between the signals and their Pearson product-moment correlation coefficient (PCC). Also, the reconstructed signals (with both the EMD and EWMD) will not be shown since they can barely be distinguished from the original ones with the naked eye.

3 Results

3.1 Accuracy of the Reconstruction

We first apply the EWMD on the two classic examples presented in [8] and for which the EMD gives accurate results. We show that our method is comparable to the EMD regarding the accuracy of the reconstruction of such signals. The first example consists of the sum of two frequency-modulated sinusoidal signals and a Gaussian wavepacket (see [8]). The signal is represented in Fig. 1 (left) with the successively extracted components with the EWMD. Though these components are

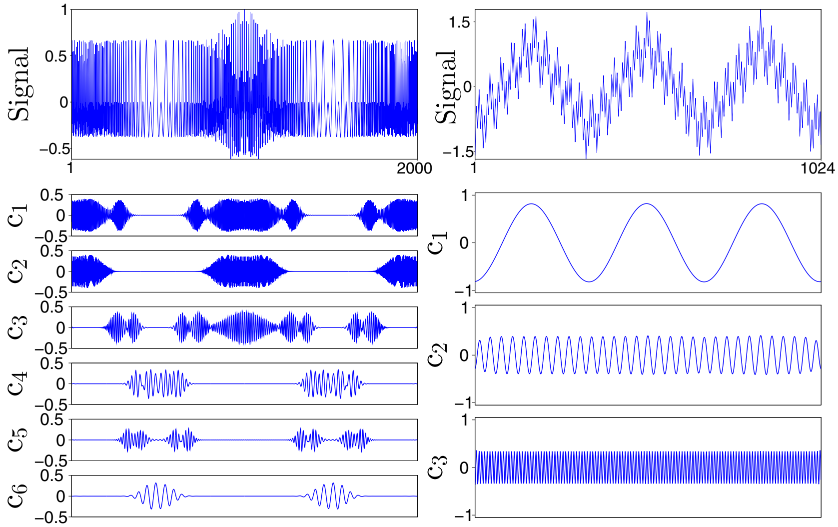

Fig. 1 Two signals analyzed with the EMD in [8] and the components extracted from the wavelet-based mode decomposition.

not the exact components of the original signal, they still manage to decompose it in an effective way. Indeed, when their sum is computed, the RMSE between the reconstructed signal and the original one is 0.086 and the PCC is 0.968. Such results are comparable to those obtained with the EMD, for which the RMSE is 0.07 and the PCC is 0.979. The second signal is the sum of a sinusoidal wave (constant frequency ω) and two triangular waveforms (one with a frequency larger than ω, the other smaller than ω). The signal and the components extracted are displayed in Fig. 1 (right). It can be seen that the three components are clearly recovered, though the triangular waveforms are somehow smoothed out. The RMSE and PCC related to the reconstructed signal compared to the original one are respectively 0.085 and 0.992, compared to 0.023 and 0.999 with the EMD. Although it seems that the EMD does a slightly better job at decomposing and reconstructing the signals, one can more than reasonably consider that the EWMD passed this test.

3.2 Period Detection Skills

One of the key features of both the EMD and wavelet decomposition is their ability to identify the periodicities hidden in a signal. In other words, they usually allow to recover the period of a sinusoidal signal as well as the mean period of an amplitude-modulated and frequency-modulated (AM-FM) signal (provided the frequency does not vary too much). Let us test the period detection skill of both methods on a toy example. We consider the signal $f(x) = \sum_{i=1}^{4} f_i(x)$ where

$$f_1(x) = \left(1 + 0.5\cos\left(\frac{2\pi}{200}x\right)\right)\cos\left(\frac{2\pi}{47}x\right) \tag{7}$$

$$f_2(x) = \frac{\ln(x)}{14}\cos\left(\frac{2\pi}{31}x\right) \tag{8}$$

$$f_3(x) = \frac{\sqrt{x}}{60}\cos\left(\frac{2\pi}{65}x\right) \tag{9}$$

$$f_4(x) = \frac{x}{2000}\cos\left(\frac{2\pi}{23 + \cos\left(\frac{2\pi}{1600}x\right)}x\right). \tag{10}$$

We thus have a signal made of three AM-components and one AM-FM component; the target periods to detect are $\approx 23, 31, 47, 65$ units. The signal and its components are plotted in Fig. 2. The successive steps (wavelet spectrum - period detection - component extraction - repeat the process) leading to the final decomposition are illustrated in Fig. 3. One can clearly notice that the extracted components match the original ones, confirming the fact that the EWMD is well-suited for that type of task. The RMSE between the reconstructed signal and f is 0.069 and the PCC is 0.996. Moreover, the periods detected by this method are 21.6, 30.6, 46.4 and 65.6 units, which are extremely close to the target periods ($\approx 23, 31, 47, 65$ units). On the other hand, the IMFs obtained with the EMD are plotted in Fig. 4. One can clearly see that they do not recover the original ones as good as the components obtained from the EWMD; it can also be noticed that the first IMF on its own is extremely similar to the signal, having alone a PCC of 0.925. Also, even though the RMSE and PCC of the reconstructed signal are still excellent (resp. 0.068 and 0.998), the periods extracted from the Hilbert-Huang transform are of ≈ 41, 75, 165, 284 units and are thus far from the expected ones.

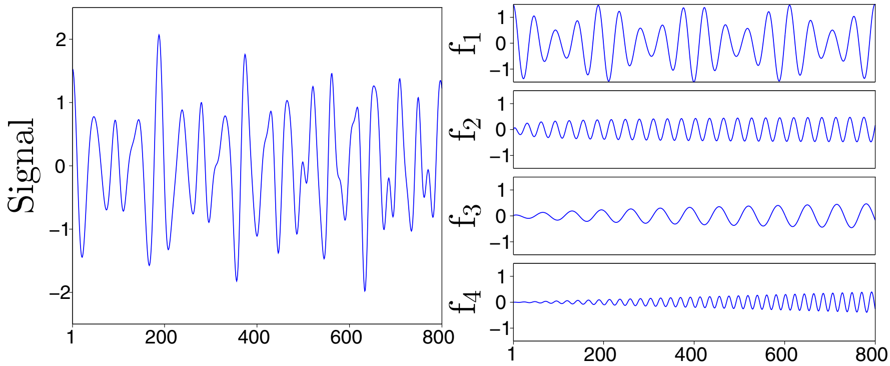

Fig. 2 The signal f (left) made of four amplitude-modulated and period-modulated components (right) used to compare the extraction and period detection skills of the EWMD and the EMD.

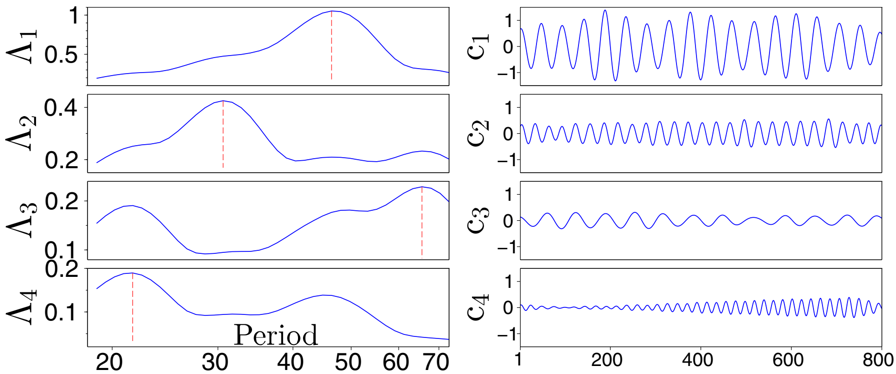

Fig. 3 Left: the wavelet spectra obtained from the successive wavelet transforms. The red dashed lines indicate where the global maximum is reached thus giving the period at which the corresponding component has to be extracted. Right: the components extracted from the wavelet transform, based on the associated wavelet spectra. The periods detected by the method are respectively (from top to bottom) 46.4, 30.6, 65.5 and 21.6 units (targets: 47, 31, 65, 23 units). The extracted components clearly match the original ones. The RMSE between the reconstructed signal and the original one is 0.069 and the PCC is 0.996.

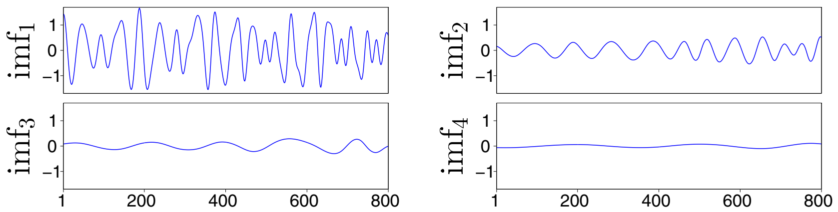

Fig. 4 The IMFs extracted from the EMD. One can see that they do not match accurately the original ones; the first IMF on its own is extremely similar to the whole signal. The periods extracted from the Hilbert-Huang transform (41, 75, 165, 284) are far from the target values (≈ 23, 31, 47, 65 units).eps

3.3 Real-Life Data: ENSO Index

The EWMD is now applied to a real-life signal. For that purpose, the El Niño Southern Oscillation (ENSO) index is analyzed (ERSST.V3B SST Niño 3.4 time series provided by the Climate Prediction Center). It is a climate pattern consisting of monthly-sampled sea surface temperature anomalies (SSTA, in Celsius degrees) in the Eastern Pacific Ocean recorded from Jan. 1950 to Dec. 2014 (see Fig. 5). An anomalous warming in the SSTA is known as El Niño, while an anomalous cooling bears the name of La Niña. ENSO is well recognized as the dominant mode of interannual variability in the tropical Pacific Ocean. It affects the atmospheric general circulation which transmits the ENSO signal to the other parts of world; these remote effects are called "teleconnections" and induce changes in the occurrence of severe weather events, which dramatically affect human activities and ecosystems worldwide (see e.g.[11, 12, 13, 14]). Therefore, the ENSO index is of primary importance for climate scientists and appears as an interesting choice for testing the EWMD.

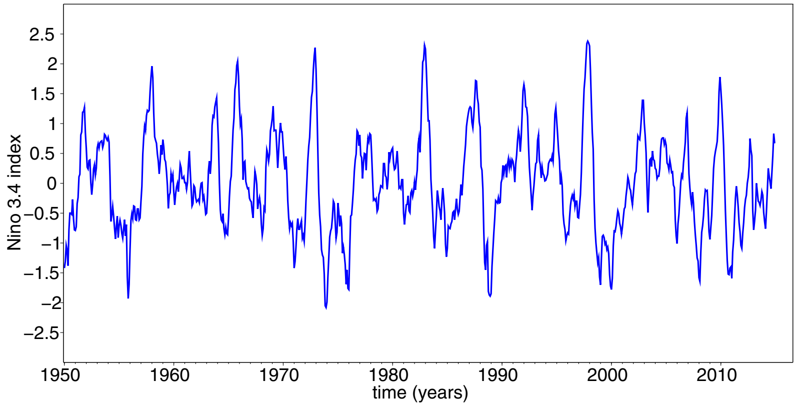

Fig. 5 The ENSO index, i.e. monthly sea surface temperature anomalies in the Equatorial Pacific Ocean.

As it can be seen in Fig. 6, the components extracted from the EWMD and the EMD are somehow comparable. The periods detected are respectively (from top to bottom in Fig. 6) 44.8, 28.6, 17, 65.6, 140.6 months for the EWMD and 9.8, 21, 38.6, 75.9, 138.4 for the EMD. It turns out that the periods detected with the EWMD seem more in agreement with previous studies than those obtained from the EMD (see e.g. [15, 16]). Let us note that both methods recover the famous $\approx$ 11-years period of the solar cycle. Regarding the reconstruction skills of the methods, the former has a RMSE of 0.277 and a PCC of 0.941, while the latter has a RMSE of 0.193 and a PCC of 0.973. Although these numbers seem to be better with the EMD, the 9.8-months component is likely a side effect due to the noise within the signal. Indeed, the EMD is known for having trouble to deal with noise, exhibiting IMFs very valuable for the reconstruction but with a rather poor physical interpretation. If that noisy component is not taken into account, the RMSE rises to 0.355 and the correlation drops to 0.903. Let us add that our first tests (not shown) indicate that the EWMD is not as sensitive to noise as the EMD, thus giving more reliable results especially for real-life data analysis. This has to be more carefully studied.

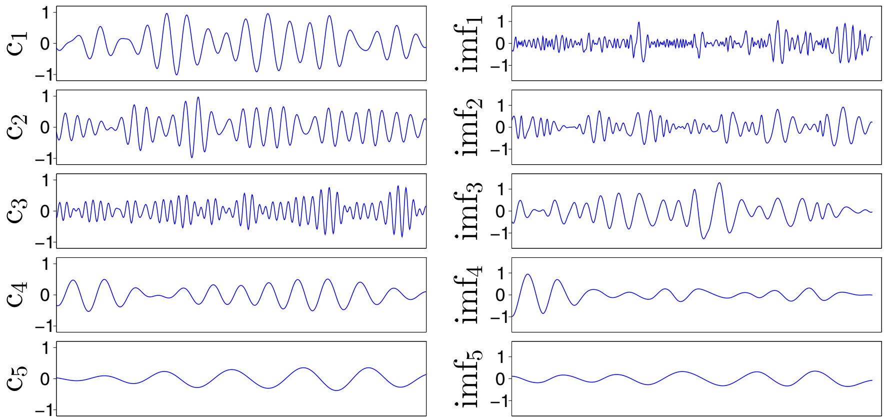

Fig. 6 Left: the components extracted from the ENSO signal with the EWMD. Right: the IMFs given by the EMD. The periods detected are 44.8, 28.6, 17, 65.6, 140.6 months (EWMD) and 9.8, 21, 38.6, 75.9, 138.4 (EMD). Those obtained with the EWMD seem to be more in agreement with some previous works. The reconstructions (not shown) are both satisfying. Let us note that the EMD displays a noisy component that artificially improves the reconstruction skills.

4 Conclusion

We presented a new wavelet-based method (EWMD) for decomposing an oscillating signal into several quasi-periodic components and compared the results with the famous empirical mode decomposition (EMD). It turns out that the decomposition-reconstruction skills of the EWMD are globally as good as those of the EMD. Moreover, the period detection abilities of the EWMD seem to outperform those of the

EMD. Regarding real-life data, we analyzed the ENSO index, i.e. temperatures of the Pacific Ocean. It appears that the periods detected by the EWMD seem more in agreement with previous studies, while both methods excel in decomposing-reconstructing the original signal. In general settings, the EWMD extracts components following somehow a decreasing level of energy while the EMD successively gives components with increasing mean frequency. Therefore, the EMD is highly sensitive to noise while the EWMD is barely affected; this should be investigated in detail in future works.

Let us note that the present paper is merely of an experimental nature and the skills of the promising EWMD have to be explored in more details. Also, we are well-aware of the fact that the EMD has been considerably improved since its first version (which is the one chosen here for comparing results). Therefore, it will be necessary to compare the EWMD with e.g. the EEMD and CEEMDAN as well as with other mode decomposition methods (such as e.g. [5] and methods mentioned therein). Let us finally note that this is the first version of the EWMD; improvements will be made in the near future, but the examples presented here show that the EWMD appears as a challenging candidate in the area of mode decomposition methods; we are optimistic about the possibilities it offers.

References

1. Nicolay, S.: A wavelet-based mode decomposition. European Physical Journal B **80**, 223–232 (2011)
2. Arneodo, A., Audit, B., Decoster, N., Muzy, J.F., Vaillant, C.: Wavelet based multifractal formalism: applications to DNA sequences, satellite images of the cloud structure, and stock market data. In: The Science of Disasters: Climate Disruptions. Heart Attacks, and Market Crashes, pp. 27–102. Springer, Berlin (2002)
3. Daubechies, I.: Ten lectures on Wavelets. SIAM (1992)
4. Mallat, S.: A Wavelet Tour of Signal Processing. Academic Press (1999)
5. Gilles, J.: Empirical wavelet transform. IEEE Transactions on Signal Processing **61**(16), 3999–4010 (2013)
6. Flandrin, P., Rilling, G., Goncalves, P.: Empirical mode decomposition as a filter bank. IEEE Signal Processing Letters **11**(2), 112–114 (2004)
7. Huang, N.E., Shen, Z., Long, S.R., Wu, M.C., Shih, H.H., Zheng, Q., Yen, N.C., Tung, C.C., Liu, H.H.: The empirical mode decomposition and the hilbert spectrum for nonlinear and non-stationary time series analysis. Proceedings of the Royal Society of London A **454**, 903–995 (1998)
8. Rilling, G., Flandrin, P., Goncalves, P.: On empirical mode decomposition and its algorithms. In: IEEE-EURASIP Workshop Nonlinear Signal Image Processing (NSIP) (2003)
9. Wu, Z., Huang, N.E.: Ensemble empirical mode decomposition: a noise-assisted data analysis method. Advances in Adaptative Data Analysis **1**, 1–41 (2009)
10. Torres, M.E., Colominas, M.A., Schlotthauer, G., Flandrin, P.: A complete ensemble empirical mode decomposition with adaptive noise. In: IEEE International Conference on Acoustic, Speech and Signal Processing (ICASSP) (2011)
11. Ashok, K., Behera, S., Rao, S., Weng, H., Yamagata, T.: El niño modoki and its possible teleconnection. Journal of Geophysical Research **112**(10.1029) (2007)
12. Glantz, M.: Currents of Change: Impacts of El Niño and La Niña on climate society. Cambridge University Press (2001)

13. Hsiang, S., Meng, K., Cane, M.: Civil conflicts are associated with the global climate. Nature **476**(7361), 438–441 (2011)
14. Yeh, S., Kug, J., Dewitte, B., Kwon, M., Kirtman, B., Jin, F.: El niño in a changing climate. Nature **461**(7263), 511–514 (2009)
15. Moron, V., Vautard, R., Ghil, M.: Trends, interdecadal and interannual oscillations in global sea-surface temperatures. Climate Dynamics **14**(7), 545–569 (1998)
16. Nicolay, S., Mabille, G., Fettweis, X., Erpicum, M.: 30 and 43 months period cycles found in air temperature time series using the morlet wavelet method. Climate dynamics **33**(7), 1117–1129 (2009)